Thermal Rectification via Heterojunctions of Solid-State Phase-Change Materials

Hyungmook Kang,[1,2] Fan Yang,[1] and Jeffrey J. Urban[1,*]

[1] *The Molecular Foundry, Lawrence Berkeley National Laboratory, Berkeley, California 94720, USA*
[2] *Department of Mechanical Engineering, University of California, Berkeley, California 94720, USA*

(Received 12 March 2018; revised manuscript received 4 June 2018; published 23 August 2018)

Nonlinear thermal transport can arise naturally in materials with strongly temperature-dependent thermal conductivities; however, this is exceedingly rare and weak. If a general strategy could be devised to yield nonlinear thermal transport, it would provide an avenue to controlling heat flow and realizing nonlinear thermal devices. Phase-change materials, which can exist in two states with distinct thermal conductivities, provide a unique opportunity to realize nonlinear thermal transport. In this work, we develop an analytical framework upon which we propose a material architecture for actualizing one type of nonlinear thermal transport, thermal rectification, where heat flux is biased in one direction. Our findings show that a heterojunction of two tunable phase-change materials can demonstrate strong thermal rectification. The magnitude of thermal rectification is analyzed as a function of the phase-change properties of each material, and we determine the fundamental heat-flux relations for each direction in these heterojunctions and criteria to separate the various phase situations that can occur. Finally, the analytical framework is applied to a junction comprising two phase-change materials, polyethylene and vanadium dioxide, and demonstrate a maximal theoretical rectification factor of approximately 140%. This analysis provides an important analytical tool in helping researchers design thermal circuits or advanced thermal energy storage media.

DOI: 10.1103/PhysRevApplied.10.024034

I. INTRODUCTION

Inspired by the conceptual keystone of the microelectronics industry, the transistor, research on thermal transport with nonlinear thermal properties, such as nonlinear temperature- (or atomic mass, pressure, geometry) dependent thermal conductivities, has attracted a great deal of attention in recent years. Thermal devices including thermal rectifiers [1–15] and thermal transistors [1,2] have been realized by nonlinear transport phenomena such as thermal rectification [i.e., heat transport characterized by a preferential direction for heat flow, as described in Fig. 1(a)]. To achieve thermal rectification, several mechanisms at solid states have been suggested, such as enhancing lattice anharmonicity [2,16], use of asymmetric nanostructures [4–9], defects in structures [10,11], and asymmetric scattering of photons [12–14]. However, none of these proposed mechanisms have yielded materials with large thermal rectification, experimentally and analytically. Another promising mechanism, solid-state junctions using phase-change materials, has been recently used for thermal rectification [17–20] and has shown great potential for making devices that scale effectively. Cottrill and Strano [21] analyzed the thermal rectification in a single phase-change material. However, they limited their analysis to the simplest case with only one phase-change material and thus can only provide rectification defined by the contrast of the high- and low-thermal-conductivity phase of that individual material. The parametric study to obtain the thermal rectification remained a numerical approach, without any empirical solution for the maximal performance. Recently, they extended the approach to a junction with two phase-change materials; however, they considered limited cases that can make only one phase-change situation at one time [22]. Ordonez-Miranda *et al*. [23] studied the added hysteresis effect of a phase-change material in the junction and figured out that the main key parameter for thermal rectification is the thermal-conductivity contrast of the phase-change material. In addition, due to the lack of choice of appropriate materials, the thermal bias spans a very broad range ($>$50 K), limiting its use in applications such as thermal-energy storage and thermal circuits, which usually operate in a narrow thermal bias. The thermal-rectification effect occurring in a narrow temperature window has a greater potential to be enhanced when the thermal bias increases.

In this paper, we propose a general theory that can handle multiple phase-change materials and interfaces, thus providing large thermal-rectification ratios well beyond

*Corresponding author. jjurban@lbl.gov

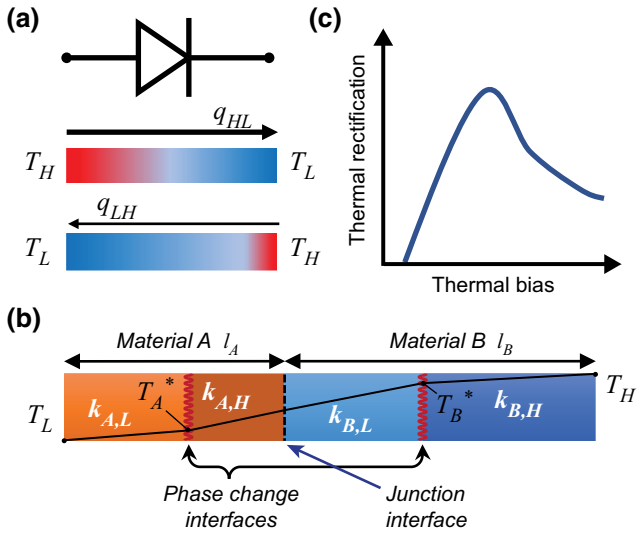

FIG. 1. Basic concept of thermal rectification and the heterojunction using two phase-change materials in series. (a) Analogous to the electrical diode, the thermal rectifier transmits heat more easily in one direction than in the reverse direction. The subscripts *HL* and *LH* indicate the direction of heat flux, from high (*H*) to low (*L*) temperature, or vice versa. (b) Schematic geometry of the suggested junction. The terminologies and symbols introduced here will be used throughout the paper. The black line represents the temperature profile within the structure when phase changes exist in both materials *A* and *B*. (c) Schematic of expected thermal rectification with respect to thermal bias via phase-change materials.

that provided by the mere thermal-conductivity contrast of any one individual material. Specifically, heterojunctions using two phase-change materials can strongly enhance the thermal rectification with the advantage of additional interfaces, as depicted in Fig. 1(b). This work encompasses a full physical picture of heat transport in phase-change materials, fundamentally addressing all possible experimentally observable scenarios of thermal rectification. This paper applies the general theory to real rapid-jump thermal-conductivity materials. With recent advancements in solid-state materials, phase transitions can occur over just a few degrees in temperature. One prominent example is the metal-insulator-transition (MIT) which occurs in tungsten-doped vanadium dioxide (VO_2) [24]. It has a MIT phase change in a very small temperature window (approximately 5 K), which can show a thermal-conductivity contrast clearly, and a higher thermal conductivity when the temperature rises across the MIT temperature. Thus, combining it with another material with the opposite temperature dependence, thermal rectification can be enhanced. Finally, the general theory suggests the theoretical maximum of the thermal-rectification factor of solid-state junctions.

II. THEORETICAL MODEL

A. Heterojunction design

We start with a junction formed by two materials, *A* and *B*, each possessing a phase change at temperatures T_A^* and T_B^*, respectively. For bulk or thin-film samples, we assume that heat transfer is a one-dimensional problem. Without losing generality, we take the case where material "B" has a higher phase-change temperature than "*A*" (i.e., $T_A^* < T_B^*$). We also assume that *A* has a thermal conductivity, $k_{A,L}$, at low temperature and a thermal conductivity, $k_{A,H}$, at high temperature. Here, the subscripts denote the material index and temperature region in relation to its phase-change temperature (higher or lower), respectively. We also apply analogous nomenclature to material *B*. For simplicity, we assume thermal conductivity is a step function with respect to temperature through the phase change. This step-function assumption is supported by the acceptable similarity of thermal conductivity trends in several materials within a large temperature range [24,25]. The schematic in Fig. 1(b) represents the geometry of the junction in materials *A* and *B* of lengths l_A and l_B, respectively. We name the heat flux traveling in the direction depicted in Fig. 1(b) as q_{LH} and the heat flux traveling in the opposite direction as q_{HL}. We treat the heat-flux directions separately, meaning q_{LH} and q_{HL} represent their absolute magnitude. With heat flux in both directions, we define the thermal-rectification factor as the normalized heat-flux difference,

$$\gamma = \frac{\max\{q_{LH}, q_{HL}\}}{\min\{q_{LH}, q_{HL}\}} - 1. \tag{1}$$

In general linear thermal transport, especially that with no thermal rectification, the thermal-rectification factor should be the minimum value, zero. The designed heterojunction would have a thermal-rectification factor trend depending on thermal bias with an maximum, as predicted in Fig. 1(c).

B. General theory results

The governing equation for this study is Fourier's law under steady-state conditions. We assume that the thermal boundary resistance at the junction is negligible. The ratio of thermal boundary resistance to the thermal resistance of materials can affect the thermal-rectification factor [22]. The eligible device length depends on the thermal conductivity of the applied materials and the contact resistance at the interface between different materials. This assumption holds if the device length is of the order of 300 nm or longer, since most similar thermal-contact conductances at the interface between different materials are of the order of 100 MW/(m^2 K) [26–28] and their minimum order is around 30 MW/(m^2 K) [29–32]. The boundary conditions are the temperatures T_H and T_L and the known phase-change temperatures T_A^* and T_B^*. Heat fluxes through each

material or phase are described by

$$-q = k_{A,L}\frac{\partial T}{\partial x}\bigg|_{T<T_A^*} = k_{A,H}\frac{\partial T}{\partial x}\bigg|_{T>T_A^*} = k_{B,L}\frac{\partial T}{\partial x}\bigg|_{T<T_B^*} = k_{B,H}\frac{\partial T}{\partial x}\bigg|_{T>T_B^*}. \quad (2)$$

The problem we consider here is a general case with two phase-change materials. When the thermal bias, $T_H - T_L$, changes, the phase-change interface in the materials moves. There are a multitude of different factors that must be taken into consideration, such as the fact that the phase change could happen in A and/or B, or the flux direction yields different amounts of heat flux. In this study, we analytically derive the heat flux for all cases, find the criteria to determine an appropriate case, compute the thermal-rectification factor γ, and give suggestions for designing an optimal thermal rectifier.

Initially, we start from the conditions that the phase-change temperatures for both materials are between T_L and T_H (i.e., $T_L \le T_A^* \le T_H$ and $T_L \le T_B^* \le T_H$). Given these conditions, there are four possible cases of heat flux for the q_{LH} direction with respect to the interface position of the phase change: a phase change occurs only in material A or B, or in both or none of the materials. Upon inspecting the opposite direction, q_{HL}, all these cases are possible except for the case of phase changes in both materials A and B due to the temperature inequality order. Through multiple steps to simultaneously solve Eq. (2) for Fourier's law, we can first derive a relation for the phase-change position in a certain material and then obtain the magnitude of steady heat flux sequentially. The general solutions to all cases in both directions are summarized in Tables I and II.

C. Criteria to determine phase situations

The criterion parameters are important since they are related to how many phase changes occur and in which material. Thus, they determine which heat-flux relation for q_{LH} in Table I or for q_{HL} in Table II is appropriate. These criterion parameters are defined by both the boundary temperatures (T_H and T_L) and the thermophysical properties of A and B. The dimensionless temperatures

$$\theta_A = \frac{T_A^* - T_L}{T_H - T_A^*} \quad \text{and} \quad \theta_B = \frac{T_B^* - T_L}{T_H - T_B^*} \quad (3)$$

are introduced as representative parameters for the thermal-condition effects on judging the cases of phase situations. The criterion for each direction is separately proposed since the possible number of phase changes is different. There are two criterion relations for each material for the q_{LH} direction. In order for a phase change to occur in material A, the temperature at the junction point between materials A and B should be larger than the phase-change temperature T_A^*. Starting from the inequality condition, we obtain the relation $1/\theta_A > R_{LH,A}$, where the dimensionless $R_{LH,A}$ is

$$R_{LH,A} = \frac{(1 - k_{B,H}/k_{B,L})(k_{A,L}l_B + k_{B,L}l_A)}{l_A(k_{B,H} + k_{B,L}\theta_B)} + \frac{k_{A,L}}{k_{B,L}}\frac{l_B}{l_A}. \quad (4)$$

Similarly, from a physical condition between T_B^* and the junction temperature, we can derive a relation detailing the existence of material B so that $\theta_B > R_{LH,B}$, where $R_{LH,B}$ is

$$R_{LH,B} = \frac{(1 - k_{A,L}/k_{A,H})(k_{A,H}l_B + k_{B,H}l_A)}{l_B(k_{A,L} + k_{A,H}/\theta_A)} + \frac{k_{B,H}}{k_{A,H}}\frac{l_A}{l_B}. \quad (5)$$

The two criteria for q_{LH} independently determine the existence of phase change in materials A and B, as summarized in Table I.

In the q_{HL} direction, one phase change can occur at most. From the same comparison, a criterion R_{HL} is found to be sufficient for determining whether or not the phase change for both materials exists:

$$R_{HL} = \frac{k_{A,H}}{k_{B,L}}\frac{l_B}{l_A}. \quad (6)$$

The detailed inequality conditions are summarized in Table II.

D. Adjustment method for extended conditions

The above criteria and the general solutions in Tables I and II are valid only when the phase-change temperatures are within boundaries $T_L \le T_A^* \le T_H$ and $T_L \le T_B^* \le$

TABLE I. Heat-flux relations for q_{LH} with corresponding criteria. The criteria in the columns and rows independently determine the existence of phase change in materials A and B, respectively.

$q_{LH} =$	Phase change in A: $1/\theta_A > R_{LH,A}$	No phase change in A: $1/\theta_A \le R_{LH,A}$
Phase change in B: $\theta_B > R_{LH,B}$	$\frac{\{k_{A,H}(T_H - T_A^*) + k_{A,L}(T_A^* - T_L)\}\{k_{B,H}(T_H - T_B^*) + k_{B,L}(T_B^* - T_L)\} + (k_{A,H} - k_{A,L})(k_{B,H} - k_{B,L})(T_H - T_B^*)(T_A^* - T_L)}{(T_H - T_L)(k_{A,H}l_B + k_{B,L}l_A)}$	$\frac{k_{A,L}\{k_{B,H}(T_H - T_B^*) + k_{B,L}(T_B^* - T_L)\}}{k_{A,L}l_B + k_{B,L}l_A}$
No phase change in B: $\theta_B \le R_{LH,B}$	$\frac{k_{B,H}\{k_{A,H}(T_H - T_A^*) + k_{A,L}(T_A^* - T_L)\}}{k_{A,H}l_B + k_{B,H}l_A}$	$\frac{k_{A,L}k_{B,H}(T_H - T_L)}{k_{A,L}l_B + k_{B,H}l_A}$

TABLE II. Heat-flux relations for q_{HL} with corresponding criteria. The relation in the second column is about the state of the absence of phase change in both materials.

	Phase change in A: $R_{HL} < \theta_A$	No change: $\theta_A \le R_{HL} \le \theta_B$[a]	Phase change in B: $\theta_B < R_{HL}$[a]
$q_{HL} =$	$\frac{k_{B,L}\{k_{A,H}(T_H - T_A^*) + k_{A,L}(T_A^* - T_L)\}}{k_{A,L}l_B + k_{B,L}l_A}$	$\frac{k_{A,H}k_{B,L}(T_H - T_L)}{k_{A,H}l_B + k_{B,L}l_A}$	$\frac{k_{A,H}\{k_{B,H}(T_H - T_B^*) + k_{B,L}(T_B^* - T_L)\}}{k_{A,H}l_B + k_{B,H}l_A}$

[a]When $\theta_B < 0$, there is no phase change in both materials. This is equivalent to assuming θ_B is a very large number.

T_H. If T_A^* or T_B^* is outside these ranges, no phase change should arise. Should this be the case, the material can be assumed to possess a constant overall thermal conductivity. To adjust the situations with correct properties, we have to substitute $k_{A,H}$ for $k_{A,L}$ and/or $k_{B,L}$ for $k_{B,H}$ to the relations and criteria for q_{LH} in Table I when $T_A^* < T_L$ and/or $T_B^* > T_H$, respectively. Likewise, when $T_A^* > T_H$ and/or $T_B^* < T_L$, the values of $k_{A,L}$ and/or $k_{B,H}$ for the q_{HL} are substituted for $k_{A,H}$ and/or $k_{B,L}$ in Table II, respectively. Another adjustment for the q_{HL} is additionally needed since R_{HL} is a single criterion for both materials, as mentioned in Table II. On the boundary of the criteria, the solutions to the heat flux of both sides should be physically continuous, and as a result, the continuity was validated.

III. CASE STUDY

A. Applied materials

Based on this general theory, we introduce a candidate material pair to show the potential thermal-rectification effect of phase-change heterojunctions. At room temperature or above, where most thermal diodes are used, low-temperature thermal conductivities in the solid-state phase are higher than the high-temperature thermal conductivities, such as for polyethylene [25] (material A in the model). To maximize the thermal rectification of the heterojunction, choosing a material with the opposite temperature trend can be a promising design for the other side. One candidate is metallic VO_2 [24] (material B in the model). Indeed, the materials have thermal conductivities in the form of a step function [24,25] and the application of the step function form has been used in the literature [21]. The narrow transition temperature range hardly degrades the thermal-rectification factor as enough thermal bias is applied [22]. The phase-change temperatures and amplitude of thermal conductivity for both materials are tunable, either by doping [24], geometric factor [25], or stress [25]. For this work, we used the thermal-conductivity data of polyethylene from large-scale molecular dynamics simulations and of metallic VO_2 [24] from experimental measurements on a suspended device. Both temperature-dependent thermal conductivities show that the shapes are good approximations to step functions even at the length scale of <100 nm. Even though VO_2 exhibits a hysteresis effect in the heating and cooling processes, the general theory can cover both the heat fluxes based on different properties from the hysteresis. Since our theory is general and we wish to test an example with more varieties of phase-change states, we assume that VO_2 has a higher value of the virtual phase-change temperature, as $T_B^* = 340$ K, than polyethylene with $T_A^* = 320$ K. Otherwise, we do not optimize other material properties (such as thermal-conductivity ratio across phase-change temperature) to achieve best performance; instead we keep them the same as the literature values [24,25], as summarized in Table III.

B. General theory results

Figure 2 shows the thermal-rectification factor dependence on thermal bias. The interface positions of phase change in both materials move with respect to the change of temperature T_H, as the temperature T_L at the other end is fixed. The moving phase-change interfaces in both materials are responsible for the various cases of thermal rectification. In the given conditions, seven distinct regions with different slopes of the thermal-rectification

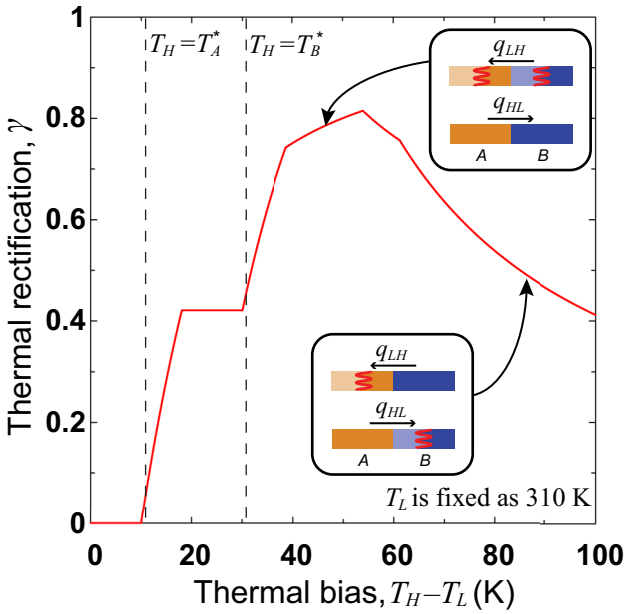

FIG. 2. Thermal-bias-dependent thermal rectification via a heterojunction between polyethylene (material A) (Ref. [25]) and tungsten-doped VO_2 (material B) (Ref. [24]) as detailed in Table III. Regimes with different slopes represent different combinations of phase-change states between the two materials Two representative states yielding different thermal-rectification trends are detailed in the inserts.

TABLE III. Material properties used for the calculation in this manuscript for polyethylene (material A) (Ref. [25]) and tungsten-doped VO_2 (material B) (Ref. [24]).

T_A^* (K)	T_B^* (K)	$k_{A,L}$ [W/(m K)]	$k_{A,H}$ [W/(m K)]	$k_{B,L}$ [W/(m K)]	$k_{B,H}$ [W/(m K)]	l_A/l_B
320	340[a]	30	10	2	4	4

[a]The value of T_B^* is virtual.

factor are observed. All are derived from different phase-change states. Two representative states, yielding different thermal-rectification trends, are described as schematics in the insets. The thermal bias determines the phase changes and thus defines the overall thermal conductivity and heat flux in each state and direction. The changing overall thermal conductivities are the underlying phenomenology behind thermal rectification.

At the flat regions in Fig. 2, we note that there is no phase change in either direction or material. The junction with two materials possessing thermally opposite phase-change trends is expected to perform high thermal rectification. In this case, the solid-state junction using the phase-change materials shows a maximal thermal-rectification factor of 80%, with a great potential to achieve higher thermal rectification when compared to the mechanism with an asymmetric shape of a material, such as the 7% of a carbon nanotube [6] and 28% of VO_2 [8]. Furthermore, as the concept developed in this work is based on bulk properties, the solid-state thermal device can be scaled up significantly more easily in comparison to the nanostructures in the literature.

The general theory presented above offers a physical interpretation of thermal rectification and thus directly examines the contribution of each parameter to the thermal-rectification factor and the relationship among these parameters. When investigating the optimization of the thermal-rectification factor according to geometric characteristics, we can recognize that the thermal rectification of the junction depends on the length ratio l_A/l_B of the materials, not on the length itself. As shown in Fig. 3, which presents the thermal-rectification factor obtained by the length ratio and thermal bias, the length ratio l_A/l_B, as a design parameter, is a critical parameter to determine the trend of the thermal-rectification factor, as well as its maximal value. Furthermore, under particular conditions, such as the black line of $l_A/l_B = 2^3$, we can observe more than one local maximum. The result with plural optimization points shows that the solid-state junction is dominated by complex phase-change scenarios and this general theory is able to provide a design guide for thermal devices from testable predictions.

IV. GLOBAL OPTIMAL SOLUTION

This general theory works as a powerful and convenient tool to understand the physics of different cases of phase change in the heterojunction and the theoretical limitations on the performance of such a thermal diode. The general theory shows that the phase-change temperature as well as the length ratio are two knobs to tune the thermal-rectification factor. In order to examine the maximum potential rectification behavior possible across the heterojunction, we study the effect that changing the phase-change temperature in each material has. In the following analysis, $T^*_{VO_2}$ is considered to be a tuning parameter while $T^*_{\text{polyethylene}}$ is fixed at 320 K; the generality of $T_A^* < T_B^*$ is kept by choosing VO_2 as material A in the cases when $T^*_{VO_2} < T^*_{\text{polyethylene}}$. Figure 4 presents the dependence of the thermal-rectification factor with respect to $T^*_{VO_2}$ for three different length ratios. The black dashed line in Fig. 4 refers to the condition where VO_2 has the same phase-change temperature as polyethylene (i.e., 320 K). Two noticeable features emerge from this analysis, which we discuss below.

Feature one is that the optimal thermal-rectification factor appears across a plateau region (and not at one particular point). The area inside the black solid line (the plateau region) has the same value of γ as a local maximum across the entire area. Basically, the highest possible γ available from the heterojunction occurs when both materials are in their most thermally conductive phase in one

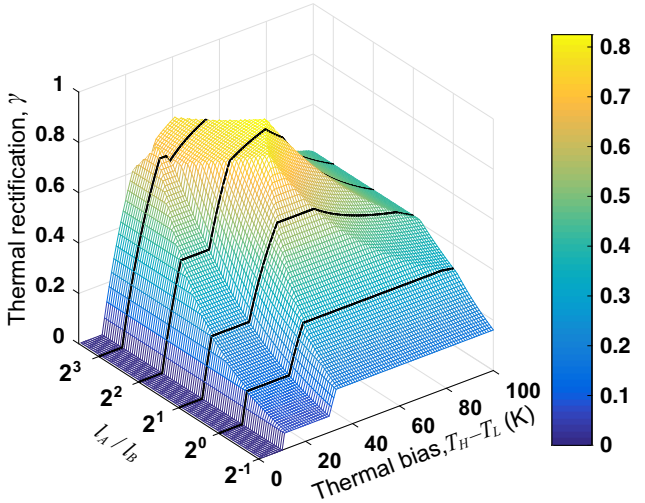

FIG. 3. Optimal thermal rectification with respect to a selected design parameter, the length ratio l_A/l_B. The 3D mesh graph shows the existence of local and general optimization points for thermal rectification. (Other parameters are detailed in Table III.)

direction and in their lowest thermally conductive phase in the other direction. However, as a practical matter, this limiting case seldom occurs in real systems, so, in general, it is important to examine the case where the local maximum γ predominates—this is where only one material exhibits a phase-change interface in both directions. In this circumstance, the plateau regions confirm that the thermal-rectification maxima are robust to small thermal perturbations from the ideal case. In more detail, when we check the phase-change states of the plateau regions, there is only one phase change in both heat-flux directions in the same material [in the VO_2 material at the length-ratio conditions of Figs. 4(a) and 4(b) and in the polyethylene material at the condition of Fig. 4(c)].

We can derive the mathematical solution of γ for each region from the general theory summarized in Tables I and II. When the phase change occurs only in material A [as is the case in Fig. 4(c) which has a large length ratio l_A/l_B], the heat flux of each direction can be calculated as

$$q_{LH} = \frac{k_{B,H}\{k_{A,H}(T_H - T_A^*) + k_{A,L}(T_A^* - T_L)\}}{k_{A,H}l_B + k_{B,H}l_A}, \quad (7)$$

$$q_{HL} = \frac{k_{B,L}\{k_{A,H}(T_H - T_A^*) + k_{A,L}(T_A^* - T_L)\}}{k_{A,L}l_B + k_{B,L}l_A}. \quad (8)$$

At conditions that cause higher heat flux in the q_{LH} direction, the solution of γ in the case of a phase change in material A in both directions can be derived by inserting Eqs. (7) and (8) into Eq. (1) as follows:

$$\gamma = \left(\frac{k_{A,L}}{k_{B,L}} + \frac{l_A}{l_B}\right) \Big/ \left(\frac{k_{A,H}}{k_{B,H}} + \frac{l_A}{l_B}\right) - 1. \quad (9)$$

Additionally, the solution of γ with a phase change in material B can be presented as

$$\gamma = \left(1 + \frac{k_{B,H}}{k_{A,H}}\frac{l_A}{l_B}\right) \Big/ \left(1 + \frac{k_{B,L}}{k_{A,L}}\frac{l_A}{l_B}\right) - 1. \quad (10)$$

Both equations are possible solutions for maximum γ, expressed as an independent relation of the thermal bias (T_H and T_L) and the phase-change temperatures (T_A^* and T_B^*). This means that the change in overall thermal conductivity for both directions is maintained at a certain rate according to the thermal bias, even though the phase-change interface is moving. Thus, the optimal plateau regions, which share an identical thermal-rectification factor, occur due to the independency of the thermal rectification on the axis variables, the thermal bias and $T_{VO_2}^*$.

The second feature worth noting arises from the fact that the thermal-bias range satisfying the local optimal γ is the widest when the phase-change temperatures of the two materials are identical, i.e., at the condition on the black dashed line in Fig. 4. As the phase-change temperatures of two materials approach the same value, the possibility of the state with two phase changes in the q_{LH} direction disappears. The more phase-change interface causes an inappropriate overall thermal conductivity in a material, and thus disturbs to actualize the higher thermal-rectification from the appropriate thermally conductive phase for each heat-flux direction. The state with only one phase change can utilize the proper phase of at least the other material in which a phase change does not occur, in contrast to the state with two phase changes. The reduced possibility of the additional phase change widens the thermal-bias condition for the local maximum γ.

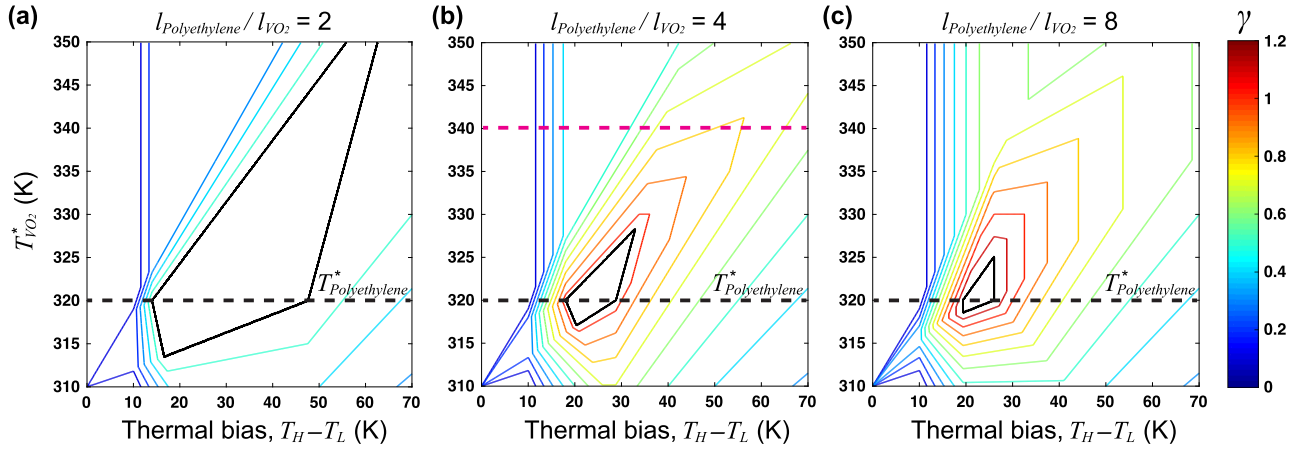

FIG. 4. Optimal thermal rectification with respect to phase-change temperature at the defined length ratio, (a) $l_{VO_2}/l_{polyethylene} = 2$, (b) $l_{VO_2}/l_{polyethylene} = 4$, and (c) $l_{VO_2}/l_{polyethylene} = 8$. The area inside the black line in each figure has the same thermal-rectification factor γ and a maximum value of γ. The black dashed lines show the conditions when VO_2 has the same phase-change temperature as polyethylene, 320 K. The magenta dashed line in (b) corresponds to the conditions of the case study in Fig. 2. (Other parameters are detailed in Table III.)

By leveraging the tunability of the phase-change temperature, a solid-state junction consisting of two materials with an identical phase-change temperature is the most promising case. Below, we examine the theoretical maximum thermal-rectification factor in this case. One additional optimization parameter for this solid-state heterojunction is the ratio of the lengths of each segment of material, l_A/l_B. Figure 5 shows the maximal thermal-rectification factor $\gamma_{\max}$ of the heterojunction at each length-ratio condition. The results of $\gamma_{\max}$ correspond to the mathematical solutions from Eq. (9) or Eq. (10), as expected from the above analysis. A global optimization value is obtainable from the intersection of the two equations. To achieve the global maximal performance of the heterojunction, the length ratio should satisfy the following relation of l_A/l_B:

$$l_A/l_B = \sqrt{\frac{k_{A,L}}{k_{B,L}}\frac{k_{A,H}}{k_{B,H}}}. \tag{11}$$

Then, when the optimized length ratio is inserted into Eq. (9) or Eq. (10), the equations result in the identical thermal-rectification factor of

$$\gamma_{\max} = \sqrt{\frac{k_{A,L}}{k_{A,H}}\frac{k_{B,H}}{k_{B,L}}} - 1. \tag{12}$$

The theoretical maximum solution is based on the geometric mean of the thermal-conductivity ratio of the two materials. The relation with the thermal-conductivity ratio is consistent with our initial intuition of selecting polyethylene as material A ($k_{A,L} > k_{A,H}$) and VO_2 ($k_{B,L} < k_{B,H}$) as material B to achieve an effect of thermal rectification in this case study. The maximum solution shows that there is no limit ceiling for the thermal rectification in this design. A phase-change material with one phase-change temperature makes two separate phases. Thus, two materials in the junction design are a sufficient number to realize the effect of thermal rectification. Additionally, we are able to check that the length ratio for the high thermal rectification is dependent on the ratio of the general thermal conductivity between two phase-change materials.

Upon close inspection of this condition of the length ratio for the theoretical maximum, a plateau region according to thermal bias does not appear; in other words, the optimum $\gamma_{\max}$ is observed at a specific thermal-bias condition. The phase-change temperature is located at the junction interface in both directions. Without any phase change in both materials, the heterojunction can be operated only with low thermal conductivities of both materials in one direction and high thermal conductivities in the opposite direction. As presented in Fig. 5, the heterojunction with the two materials has a theoretical potential to present a $\gamma_{\max}$ of over 140%. Although based on optimal phase-change temperatures of materials and a specific thermal-bias condition, the theoretical maximum value suggests guidance for design and material selection, and clarifies the possibility of the heterojunction as a thermal rectifier with an outstanding thermal-rectification factor.

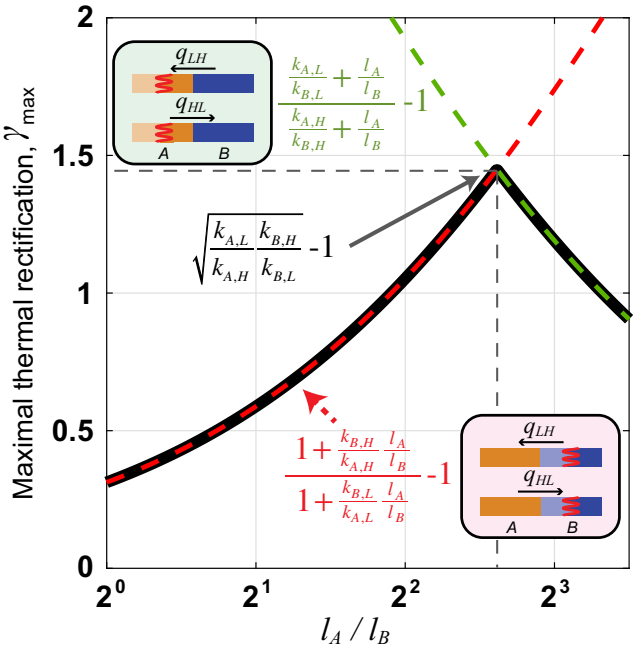

FIG. 5. Maximal thermal rectification $\gamma_{\max}$ with the $T_A^* = T_B^*$ condition at each length ratio. The green line is the solution of γ for the case of a phase change in material A in both directions and the red line is the solution for that in material B. The global maximal rectification is observed at the intersection between the two solutions. The theoretical maximal rectification is based on the geometric mean of the thermal-conductivity ratio of the two materials, expressed as $\sqrt{(k_{A,L}/k_{A,H})(k_{B,H}/k_{B,L})} - 1$, with the optimized length ratio of $l_A/l_B = \sqrt{(k_{A,L}/k_{B,L})(k_{A,H}/k_{B,H})}$. (Other parameters are detailed in Table III.)

V. CONCLUSION

In summary, we discuss a general theory for calculating thermal rectification of a solid-state junction comprising two phase-change materials. This provides a comprehensive analysis, considering whether phase changes happen in either (or both) of two material heterojunctions. The analysis of a heterojunction by the general theory shows the possibility to obtain a high thermal rectification. With a further analysis based on the tunable phase-change materials, the general theory suggests the theoretical maximal thermal-rectification factor from an optimization of design and thermal-bias conditions. We believe that the methodology in this work provides an effective way to explore the application of thermal rectification to a nonlinear thermal device.

ACKNOWLEDGMENTS

The work at the Molecular Foundry was supported by the Office of Science, Office of Basic Energy Sciences, at the U.S. Department of Energy (DOE), Contract No. DE-AC02-05CH11231. H.K. gratefully acknowledges financial support from Kwanjeong Educational Foundation. We are indebted to M. P. Gordon and W. Lee for critical reading of the manuscript.

[1] N. Li, J. Ren, L. Wang, G. Zhang, P. Hänggi, and B. Li, Colloquium: Phononics: Manipulating heat flow with electronic analogs and beyond, Rev. Mod. Phys. **84**, 1045 (2012).

[2] N. Yang, N. Li, L. Wang, and B. Li, Thermal rectification and negative differential thermal resistance in lattices with mass gradient, Phys. Rev. B **76**, 020301 (2007).

[3] M. Peyrard, The design of a thermal rectifier, Europhys. Lett. **76**, 49 (2006).

[4] N. A. Roberts and D. Walker, A review of thermal rectification observations and models in solid materials, Int. J. Therm. Sci. **50**, 648 (2011).

[5] Y. Wang, A. Vallabhaneni, J. Hu, B. Qiu, Y. P. Chen, and X. Ruan, Phonon lateral confinement enables thermal rectification in asymmetric single-material nanostructures, Nano Lett. **14**, 592 (2014).

[6] C. Chang, D. Okawa, A. Majumdar, and A. Zettl, Solid-state thermal rectifier, Science **314**, 1121 (2006).

[7] B. V. Budaev and D. B. Bogy, Thermal rectification in inhomogeneous nanotubes, Appl. Phys. Lett. **109**, 231905 (2016).

[8] J. Zhu, K. Hippalgaonkar, S. Shen, K. Wang, Y. Abate, S. Lee, J. Wu, X. Yin, A. Majumdar, and X. Zhang, Temperature-gated thermal rectifier for active heat flow control, Nano Lett. **14**, 4867 (2014).

[9] T. Zhang and T. Luo, Giant thermal rectification from polyethylene nanofiber thermal diodes, Small **11**, 4657 (2015).

[10] H. Wang, S. Hu, K. Takahashi, X. Zhang, H. Takamatsu, and J. Chen, Experimental study of thermal rectification in suspended monolayer graphene, Nat. Commun. **8**, 15843 (2017).

[11] R. Dettori, C. Melis, R. Rurali, and L. Colombo, Thermal rectification in silicon by a graded distribution of defects, J. Appl. Phys. **119**, 215102 (2016).

[12] Z. Chen, C. Wong, S. Lubner, S. Yee, J. Miller, W. Jang, C. Hardin, A. Fong, J. E. Garay, and C. Dames, A photon thermal diode, Nat. Commun. **5**, 5446 (2014).

[13] P. Ben-Abdallah and S.-A. Biehs, Phase-change radiative thermal diode, Appl. Phys. Lett. **103**, 191907 (2013).

[14] A. Ghanekar, J. Ji, and Y. Zheng, High-rectification near-field thermal diode using phase change periodic nanostructure, Appl. Phys. Lett. **109**, 123106 (2016).

[15] C. Dames, Solid-state thermal rectification with existing bulk materials, J. Heat Transf. **131**, 061301 (2009).

[16] D. M. Leitner, Thermal boundary conductance and thermal rectification in molecules, J. Phys. Chem. B **117**, 12820 (2013).

[17] W. Kobayashi, Y. Teraoka, and I. Terasaki, An oxide thermal rectifier, Appl. Phys. Lett. **95**, 171905 (2009).

[18] D. Sawaki, W. Kobayashi, Y. Moritomo, and I. Terasaki, Thermal rectification in bulk materials with asymmetric shape, Appl. Phys. Lett. **98**, 081915 (2011).

[19] W. Kobayashi, D. Sawaki, T. Omura, T. Katsufuji, Y. Moritomo, and I. Terasaki, Thermal rectification in the vicinity of a structural phase transition, Appl. Phys. Express **5**, 027302 (2012).

[20] R. Chen, Y. Cui, H. Tian, R. Yao, Z. Liu, Y. Shu, C. Li, Y. Yang, T. Ren, and G. Zhang, Controllable thermal rectification realized in binary phase change composites, Sci. Rep. **5**, 8884 (2015).

[21] A. L. Cottrill and M. S. Strano, Analysis of thermal diodes enabled by junctions of phase change materials, Adv. Energy Mater. **5**, 1500921 (2015).

[22] A. L. Cottrill, S. Wang, A. T. Liu, W. J. Wang, and M. S. Strano, Dual phase change thermal diodes for enhanced rectification ratios: Theory and experiment, Adv. Energy Mater. **8**, 1702692 (2018).

[23] J. Ordonez-Miranda, J. M. Hill, K. Joulain, Y. Ezzahri, and J. Drevillon, Conductive thermal diode based on the thermal hysteresis of VO_2 and nitinol, J. Appl. Phys. **123**, 085102 (2018).

[24] S. Lee, K. Hippalgaonkar, F. Yang, J. Hong, C. Ko, J. Suh, K. Liu, K. Wang, J. J. Urban, and X. Zhang, Anomalously low electronic thermal conductivity in metallic vanadium dioxide, Science **355**, 371 (2017).

[25] T. Zhang and T. Luo, High-contrast, reversible thermal conductivity regulation utilizing the phase transition of polyethylene nanofibers, ACS Nano **7**, 7592 (2013).

[26] D.-W. Oh, C. Ko, S. Ramanathan, and D. G. Cahill, Thermal conductivity and dynamic heat capacity across the metal-insulator transition in thin film VO_2, Appl. Phys. Lett. **96**, 151906 (2010).

[27] M. D. Losego, L. Moh, K. A. Arpin, D. G. Cahill, and P. V. Braun, Interfacial thermal conductance in spun-cast polymer films and polymer brushes, Appl. Phys. Lett. **97**, 011908 (2010).

[28] D. G. Cahill, W. K. Ford, K. E. Goodson, G. D. Mahan, A. Majumdar, H. J. Maris, R. Merlin, and S. R. Phillpot, Nanoscale thermal transport, J. Appl. Phys. **93**, 793 (2003).

[29] M. D. Losego, M. E. Grady, N. R. Sottos, D. G. Cahill, and P. V. Braun, Effects of chemical bonding on heat transport across interfaces, Nat. Mater. **11**, 502 (2012).

[30] S. Majumdar, J. A. Sierra-Suarez, S. N. Schiffres, W.-L. Ong, C. F. Higgs III, A. J. McGaughey, and J. A. Malen, Vibrational mismatch of metal leads controls thermal conductance of self-assembled monolayer junctions, Nano Lett. **15**, 2985 (2015).

[31] H. Acharya, N. J. Mozdzierz, P. Keblinski, and S. Garde, How chemistry, nanoscale roughness, and the direction of heat flow affect thermal conductance of solid–water interfaces, Ind. Eng. Chem. Res. **51**, 1767 (2011).

[32] H. D. Pandey and D. M. Leitner, Influence of thermalization on thermal conduction through molecular junctions: Computational study of PEG oligomers, J. Chem. Phys. **147**, 084701 (2017).